Available online at www.sciencedirect.com
ScienceDirect
Journal of Power Sources 172 (2007) 180–188
JOURNAL OF POWER SOURCES
www.elsevier.com/locate/jpowsour

Electrooxidations of ethanol, acetaldehyde and acetic acid using PtRuSn/C catalysts prepared by modified alcohol-reduction process

Gang Wu [a,*], Raja Swaidan [b], Guofeng Cui [c]

[a] *Department of Chemical Engineering, University of South Carolina, Columbia, SC 29208, USA*
[b] *Department of Chemical Engineering, Cooper Union, New York, NY 10003, USA*
[c] *School of Chemistry and Chemical Engineering, Sun-Yat Sen University, Guangzhou 510275, China*

Received 4 June 2007; received in revised form 17 July 2007; accepted 18 July 2007
Available online 25 July 2007

Abstract

Well-dispersed ternary PtRuSn catalysts of various atomic ratios (60:30:10, 60:20:20 and 60:10:30) were deposited onto carbon using modified alcohol-reduction process for electrochemical oxidation of ethanol. The alloy phase structure and surface morphology for each variation of the PtRuSn/C catalysts were determined by XRD and HRTEM. In order to evaluate the contributions of Ru and Sn in the different stages of ethanol oxidation, electrochemical oxidations of adsorbed CO, ethanol, acetaldehyde and acetic acid were performed on each PtRuSn/C catalyst. The results indicated that the Ru-rich PtRuSn/C catalyst (60:30:10) exhibited the lowest onset potential for the electrooxidations of adsorbed CO, ethanol and acetaldehyde, revealing that the removal through oxidation of the intermediate C_1 and C_2 species from Pt sites is primarily attributed to the Ru and Pt_3Sn alloy structures. However, for the overall oxidation of ethanol, the Sn-rich PtRuSn/C catalyst (60:10:30) containing PtSn phase and SnO_2 structure is favorable for the activation of C–C bond breaking, thereby generating higher current density (mass activity) at higher potentials. Moreover, in the electrooxidation of acetic acid, a remarkable improvement for oxidizing acetic acid to C_1 species was observed in the Sn-rich PtRuSn/C catalyst (60:10:30), while the Ru-rich PtRuSn/C catalyst (60:30:10) was almost incapable of breaking the C–C bond to further oxidize acetic acid. The possible reasons for the different reactivities on the studied PtRuSn/C catalysts were discussed based on the removal of intermediates and activation of the C–C bonds on the different surfaces.

Keywords: PtRuSn/C; Ethanol electrooxidation; Acetaldehyde electrooxidation; Acetic acid electrooxidation; Direct ethanol fuel cell

1. Introduction

The development of a direct alcohol fuel cell (DMFC) for which the fuel is fed directly as an alcohol solution has increased interest in the electrochemical oxidation of alcohol [1–3]. Direct injection of the alcohol fuel would avoid the problems related to the production, purification and storage of hydrogen. Though methanol is the easiest to completely oxidize to CO_2, ethanol has become a more attractive candidate as it can be produced in great quantities from biomass and is less toxic than methanol [4]. In addition, the option of using ethanol can relieve the crossover of alcohol through the membrane from anode to cathode, a phenomena leading to a mixed potential observed in the oxygen reduction reaction that decreases energy efficiencies [5]. However, the complete oxidation of ethanol to CO_2 with a release of 12 electrons at temperatures compatible with available membranes is the major challenge in the electrocatalysis process due to the lack of sufficiently active and selective electrocatalysts [6].

Indeed, in the electrooxidation of methanol, it is well known that Ru is often added to Pt to decrease this poisoning effect of CO adsorption on Pt. The Ru is thought to take part in a bifunctional mechanism and produce a ligand effect, such that some Ru atoms exist as oxidized Ru supplying the oxygenated species necessary for complete oxidation of methanol to CO_2 and other Ru atoms alloy with Pt allowing the weakening of the Pt–CO bond [7]. In the case of ethanol as the fuel in a direct ethanol fuel cell (DEFC), the issue is further complicated because ethanol contains two atoms of carbon. Therefore, a good electrocatalyst toward the complete oxidation of ethanol to CO_2 must not only avoid the poisoning of the catalytic surface by CO species as occurs with methanol oxidation but must also activate the C–C bond breaking [8,9].

* Corresponding author. Tel.: +1 803 7777238; fax: +1 803 7778265.
E-mail address: wugang@engr.sc.edu (G. Wu).

0378-7753/$ – see front matter © 2007 Elsevier B.V. All rights reserved.
doi:10.1016/j.jpowsour.2007.07.034

Previous studies on ethanol electrooxidation showed that some bimetallic catalysts such as PtRu [10–14] and PtSn [15–18] can lower the onset potential of ethanol oxidation and increase the current density as compared to Pt electrodes. Moreover, the catalytic activity and selectivity for ethanol oxidation are depended on the composition and structure in these bimetallic catalysts. Iwasita and coworkers [11] found that the optimum Ru concentration in PtRu/C catalyst towards the ethanol oxidation reaction is in a narrow of ca. 37–40%. The maximum can be explained as being caused by two opposite Ru effects: the positive effect of favoring C_1 and C_2 intermediate oxidation and the apparent negative effect of inhibiting ethanol adsorption due to the diminution of neighboring Pt sites, which are necessary to adsorb the molecule and break the C–C bond. As for the PtSn/C catalysts, Lamy and coworkers [19] indicated that the addition of Sn favors the dissociative adsorption of ethanol, which leads to the breaking of the C–C bond with a higher selectivity than that observed on the pure Pt. This conclusion was supported by IR data. Moreover, the enhancement also depends on the potentials of the reaction as well as the optimal distribution of Sn between the alloyed and non-alloyed states. At low potentials, the electrooxidation of ethanol is not fast, the oxidations of adsorbed CO and CH_3CO species determine the rate of the process. In this case, the oxidation of ethanol is enhanced by the presence of tin oxides. On the other side, at high potentials, the oxidation of ethanol increases with the increase of the lattice parameter, which is associated with an increased number of Pt–Sn pairs and is necessary to complete the oxidation of ethanol [20].

However, although it is evidenced that the overall kinetics can be improved by using bimetallic Pt-based electrocatalysts, the incomplete ethanol oxidation also prevails on these binary catalysts. Adsorbed C_2 hydrocarbon residues have been identified as major adsorbed intermediates by means of differential electrochemical mass spectrometry (DEMS) [21,22] and in situ infrared spectroscopy [22,23]. Acetaldehyde and acetic acid have been detected as the main by-products. Thus, although there is agreement that PtRu and PtSn are more active for the oxidation of ethanol, the effect of the second metal (Ru and Sn) does not seem to be similar in each case. Further study is necessary to reap the beneficial effects of each metal in improvement of the activity and selectivity for the reaction.

Considering the beneficial combination of Ru and Sn, ternary PtRuSn/C catalysts of various atomic ratios (60:30:10, 60:20:20 and 60:10:30) were synthesized to simultaneously promote the removal of adsorbed intermediate and the activation of the C–C bond breaking. Furthermore, to gain a better understanding the roles of Ru and Sn in the different stages of ethanol oxidation, electrooxidations of the adsorbed CO, ethanol, acetaldehyde and acetic acid were compared over the PtRuSn catalysts with various compositions.

2. Experimental

2.1. Catalyst synthesis

Carbon supported ternary PtRuSn catalysts with constant total metal loading of 20 wt.% with varying Pt:Ru:Sn atomic ratios of 60:30:10, 60:20:20 and 60:10:30 were synthesized by a modified alcohol-reduction process. Here, the amount of Pt is kept constant while those of Ru and Sn are varied to investigate their roles in the ethanol oxidation process.

The commercially available Ketjen Black EC 300J carbon black materials were adopted as carbon supports. This kind of carbon materials are oil furnace blacks having a B.E.T. surface area of about 950 $m^2\,g^{-1}$ and containing a large fraction of mesophase carbon. The support material has regions of long-range order with more corrosion resistance [24].

The alcohol-reduction method [25] was modified to synthesize the PtRuSn/C catalysts. Briefly, H_2PtCl_6, $RuCl_3$ and $SnCl_2$, used as metal precursors with required atomic ratios (nominal Pt:Ru:Sn = 60:30:10, 60:20:20 and 60:10:30) were dissolved in ethylene glycol under vigorous stirring for 30 min to form a solution. Subsequently, the pH of the solution was raised to above 12.0 by addition of 1 M NaOH solution and then the temperature was increased to 130 °C and kept constant for 2 h. Ultrasonically dispersed carbon slurry was added and 4 h were allotted to the impregnation of the carbon particles. The resulting mixture was cooled down to room temperature, filtered and washed by ethanol solution. Finally, the precipitate was heat treated at 400 °C for 1 h under the Ar–H_2(5%) atmosphere.

2.2. Physical characteristics

X-ray diffraction (XRD) patterns were recorded by a Bruker d8 diffractometer equipped with a Cu Kα radiation and a graphite monochromatic operation at 45 kV and 40 mA. The diffraction patterns were scanned at a rate of 1.2° min^{-1} with a scan step of 0.02°.

HRTEM images were taken on JEOL JEM-2010F with a resolution of 0.102 nm operating at 200 kV. The real atomic ratios of the PtRuSn/C catalysts were analyzed by the energy dispersive X-ray spectroscopy (EDS) technique coupled to the HRTEM.

2.3. Electrochemical measurement

Electrochemical experiments were performed in a conventional three-electrode cell using an EG&G Parc M273 potentiosate. A rotating disk electrode (RDE) with a glassy carbon disk (5 mm o.d.) was used as the working electrode. Pt wire and a standard $Hg/HgSO_4$ (0.64 V versus NHE) were used as the counter and reference electrode, respectively.

In a CO stripping measurement, the H_2SO_4 solutions were first purged with nitrogen for 20 min. CO was bubbled in and excess CO was removed from the solution by purging with nitrogen again for 20 min. The CO stripping CV curve and blank CV curve were obtained from two successive cycles recorded in the potential between 0 and 1.0 V at a sweep rate of 10 mV s^{-1}.

Electrooxidation of ethanol on the PtRuSn/C catalysts was examined in 0.5 M CH_3CH_2OH + 0.5 M H_2SO_4 solutions by a CV technique at a sweep rate of 10 mV s^{-1} between 0 and 1.0 V at room temperature. Moreover, in order to determine the effects of Ru and Sn contents on the different stages in the overall ethanol process, the oxidations of acetaldehyde and acetic acid also were examined in 0.25 M CH_3CHO + 0.5 M H_2SO_4

and 0.25 M CH_3COOH + 0.5 M H_2SO_4 solutions, respectively, at a sweep rate of 10 mV s^{-1} and room temperature.

3. Results and discussion

3.1. Physical characterizations of PtRuSn/C catalysts

3.1.1. XRD analysis

XRD patterns for the PtRuSn/C catalysts with various atomic ratios are shown in Fig. 1, along with the pattern for a Pt/C catalyst prepared using the same procedure. All the XRD patterns clearly show the three main characteristic peaks of the face-centered cubic (fcc) crystalline Pt, namely, the planes (1 1 1), (2 0 0), (2 2 0), demonstrating that all the PtRuSn/C catalysts mainly resemble the single-phase disordered structure. It should be noticed that these peaks slightly shifted to lower 2θ values for the PtRuSn catalysts as compared to those of the Pt/C catalyst. In principle, the 2θ angle shifts of the crystalline Pt peaks reveal the formation of an alloy caused by the incorporation of Ru and Sn into the fcc structure of Pt. It was reported [26] that the lattice parameter for the PtRu alloy catalyst which has higher 2θ values than Pt, is smaller than that of Pt. This indicates a contraction of the lattice after alloying. However, the lattice parameter of PtSn catalyst, which shows lower 2θ values, is larger than that of pure Pt. Therefore, the lower 2θ values observed for the PtRuSn/C catalysts are due to an overwhelming influence of the Sn atoms incorporated into the Pt structure. The Pt–Sn alloy contents are dominant with respect to the Pt–Ru alloy in the studied PtRuSn/C catalysts. It also can be found that the shift value of 2θ increases with increasing Sn content in the catalysts, as more Sn atoms are incorporated into Pt fcc structures.

In addition, the peaks located at 29.9, 34.6, 38.8 and 45.5 assigned to the alloy phase Pt_3Sn (JCPDS No. 35-1360) are observed in the PtRuSn/C (60:30:10) catalyst. However, the PtSn alloy phase (JCPDS No. 25-614) corresponded to the peaks at 26.2, 31.1, 42.3, 44.5 were detected in the PtRuSn/C with higher Sn contents (60:20:20 and 60:10:30). Thus at the low Sn contents, the Pt_3Sn phase is easier to form, and an increase in the Sn content will prompt the main alloy structure to change to the PtSn phase. As for CO stripping over the PtSn/C catalyst, it had already been indicated that oxidation of the CO adsorbed on Pt sites is promoted by the adjacent Sn atoms in the Pt_3Sn alloy [27]. On the other hand, the amount of Ru or Sn alloyed with Pt usually is smaller than nominally predicted, because some of these atoms are present as amorphous species on the catalyst surface, most likely as oxides [28]. So, as expected, Sn will exist in part as the SnO_2 (JCPDS No. 21-1250) surrounding Pt alloy, which was confirmed by the XRD pattern at the 2θ value of 33.1 and 52.1 in the Sn-rich PtRuSn/C catalyst (60:10:30).

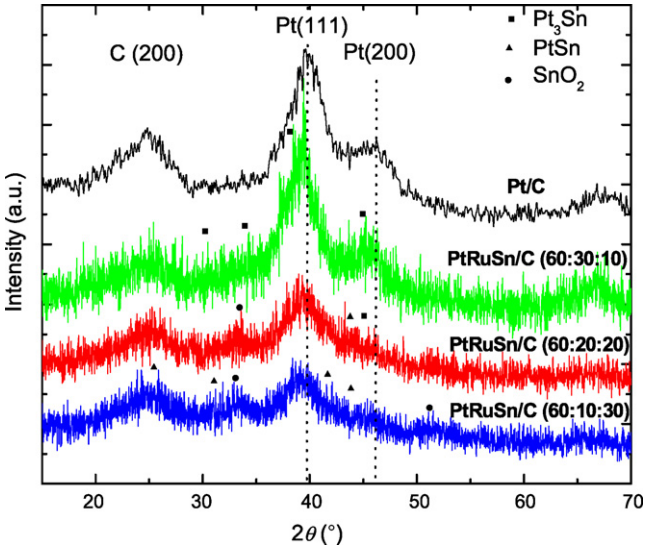

Fig. 1. X-ray diffractogram of Pt/C and PtRuSn/C electrocatalysts prepared by modified alcohol reduction.

3.1.2. HRTEM and EDX analysis

The carbon-supported PtRuSn catalysts prepared by the modified alcohol reduction with various atomic ratios were analyzed for nanoparticle size, distribution, morphology and actual composition using HRTEM and EDS. Fig. 2(a), (c) and (e) presents the results of the low-magnification HRTEM analysis of the PtRuSn catalysts with nominal 60:30:10, 60:20:20 and 60:10:30 atomic ratios, respectively. It can be seen that the mean size for these nanoparticles determined by averaging 100 particles at random is slightly larger with increasing content of Sn from about 3.2 nm for 60:30:10 to about 4.8 nm for 60:10:30. A similar trend was also observed in the case of PtSn/C catalysts [15]. Moreover, these images show that the distribution of the metal particles on the carbon support is uniform and in a narrow particle size range for all the samples. The uniformity of catalyst particle distribution is known to be important for electrocatalytic activity.

Fig. 2(b), (d) and (f) shows the high-magnification HRTEM images for the three PtRuSn/C catalysts. The two-dimensional projections reveal that all the particles appear in the asymmetric faceted shape of Pt alloy particles. It has been reported [29] that the Pt_3Sn, PtSn and SnO_2 phases are nearly cubic, hexagonal and tetragonal, respectively. Comparing the HRTEM images of the PtRuSn/C catalysts, the phase structures onto the catalyst surface also can be approximately identified. It was found that the particle shape of PtRuSn/C catalyst with the 60:30:10 atomic ratio belong to the cubic Pt_3Sn phase, while in the case of 60:10:30, the particles appear in the hexagonal shape of the PtSn phase. Furthermore, comparison of the catalyst of atomic ratio 60:10:30 with the other PtRuSn/C catalysts reveals some amorphous phases in the vicinity of Pt particles, as indicated by the arrow. The XRD analysis helps to identify this amorphous phase as SnO_2. In addition, from the HRTEM images, the Pt(1 1 1) spacing also was elongated clearly from the nominal Pt(1 1 1) spacing of 0.226 nm (PCPDF#040802) to 0.236 nm for the PtRuSn/C (60:10:30), which is in good agreement with the XRD analysis.

The EDS analysis coupled with the HRTEM indicated the real compositions for Pt:Ru:Sn in these ternary catalysts as 61:28:11, 63:18:19 and 64:9:27, which are very close the nominal atomic ratios of 60:30:10, 60:20:20 and 60:10:30, respectively. We therefore still use the nominal value to label these catalysts.

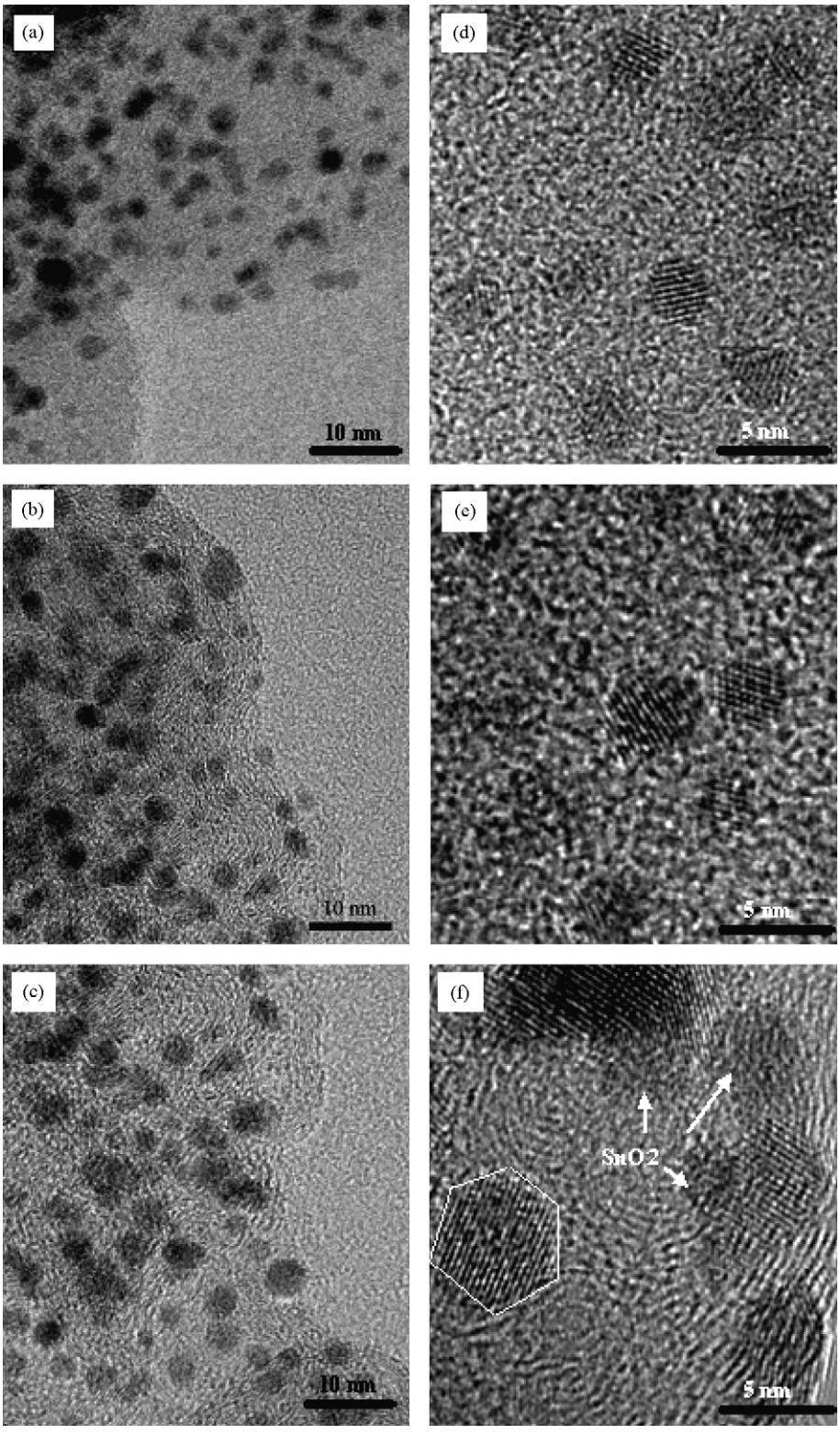

Fig. 2. HRTEM micrographs at low and higher magnifications for PtRuSn/C synthesized via modified alcohol-reduction method with various atomic ratios of 60:30:10 (a and d), 60:20:20 (b and e) and 60:10:30 (c and f).

3.2. CV characteristics and CO stripping for PtRuSn/C catalysts

The CO-stripping experimentation presents an effective method to evaluate the tolerance of adsorbed CO_{ad} poison onto the Pt-based electrocatalysts in the alcohol electrooxidation process. A CO-stripping and subsequent background voltammograms were recorded in 0.5 M H_2SO_4 solution at a sweep rate of 10 mV s^{-1} and shown in Fig. 3. The result of Pt/C was also included in this figure for comparison.

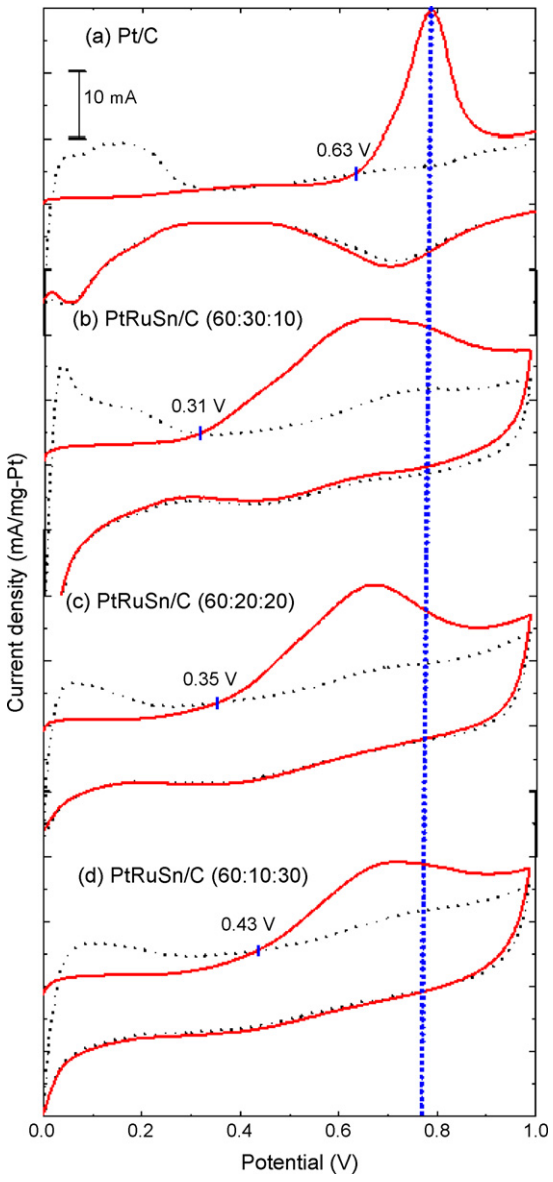

Fig. 3. CO stripping voltammograms on PtRuSn/C and Pt/C catalysts recorded at a sweep rate of 10 mV s^{-1} in 0.5 M H_2SO_4 solutions. The dashed lines refer to the blank curves after CO stripping.

It was seen in the blank background CV curves (dashed line) that all PtRuSn/C samples show the well-known hydrogen adsorption/desorption characteristics for Pt usually assigned to weakly and strongly bonded hydrogen with positive increasing adsorption or desorption potential, respectively. As evidenced by the hydrogen desorption peaks, the ratio of strongly to weakly bonded adsorbed on the PtRuSn/C (60:10:30) is higher than that of other samples. According to Beden and coworkers [30], alcohol molecule preferentially adsorbs on the Pt sites, where can strongly bind hydrogen. Hence, it can be deduced that when the number of sites capable of strong hydrogen adsorption increases, the ethanol oxidation activity is also enhanced. Hence, the results indicated that the adsorption of ethanol molecule is more easily accomplished on the PtRuSn/C (60:10:30) than on other catalysts. In addition, the background current of PtRuSn/C catalyst in the intermediate potential region (0.35–0.6 V), associated with the double-layer capacitance of the electrode is much higher than that of Pt/C, due to the formation of compact Ru and Sn oxide [31]. In the CO-stripping experiment, the disappearance of the hydrogen adsorption peaks at low potentials indicates the blocking of the hydrogen adsorption sites by adsorbed CO. The oxidation of an adsorbed CO monolayer starts from 0.62 V (onset potential) in a narrow current peak with a maximum at 0.75 V over Pt/C catalyst, while in the case of the PtRuSn/C catalysts, the CO oxidation peak become broader with significant lower onset potentials appearing at between 0.31 and 0.43 V. In particular, it is noticeable that the PtRuSn/C (60:30:10) catalyst exhibited the lowest onset (0.31 V) and peak (0.65 V) potentials and also showed the highest area specific activity for the electrooxidation of CO. With the decreasing of Ru to 10% in the PtRuSn/C catalysts (60:10:30), it was found that the onset potential positively shifts to 0.43 V. This suggests a weakening in the ability to oxidize and remove the adsorbed CO from Pt sites on Sn-rich PtRuSn/C catalyst due to the lack of available Ru.

Previous results also proposed that Ru is most successful in oxidation and removal of the CO_{ad} that is strongly bound on Pt, primarily because it serves as an oxygen source Ru–OH_{ad} at relative low potentials—and also because it contributes to changing the electronic structure of the Pt alloy (ligand effect). Despite reports that Sn can supply the OH to improve the oxidation of CO_{ad}, it has been proposed that the electroactivity of PtSn/C catalyst is proportional to the amount of Pt_3Sn phase present without any contribution for CO oxidation derived from the PtSn phase, Pt/SnO_2 clusters or other structures [28]. As a result, the Ru-rich PtRuSn/C catalyst (60:30:10) exhibits the best activity to oxidize adsorbed CO may be partially attributed to the highest Ru content and also to the abundant Pt_3Sn structures in the catalyst, which was confirm by XRD analysis.

3.3. Electrooxidation of ethanol, acetaldehyde and acetic over PtRuSn/C catalysts

3.3.1. Electrooxidation of ethanol

Fig. 4 shows the cyclic voltammograms for ethanol oxidation in 0.5 M H_2SO_4 + 0.5 M CH_3CH_2OH at room temperature over PtRuSn/C catalysts with various atomic ratios of 60:30:10, 60:20:20 and 60:10:30. The Pt content is kept constant in these catalysts to easily understand the relative contributions of Ru and Sn in the different stages of ethanol oxidation process. Comparison of CV curves for ethanol oxidation indicated that the Ru-rich PtRuSn/C catalyst (60:30:10) exhibits the lowest onset potential (0.22 V). When the Ru contents decrease, the onset potentials positively shifted to 0.29 and 0.26 V for the cases of 60:20:20 and 60:10:30 atomic ratios, respectively. The onset potentials for Pt/C, PtSn/C and PtRu/C catalysts in the ethanol oxidation reaction were previously reported [20] ca. 0.38, 0.30 and 0.27 V, respectively. The same order was also observed by Zhou et al. [32]. Generally, compared with the binary PtRu/C and PtSn/C, the ternary PtRuSn/C catalysts can further shift the onset potential to the negative direction by 50–80 mV depending on the catalyst compositions. The relatively positive shifts onset potentials observed with Sn contents in the PtRuSn/C catalysts are due

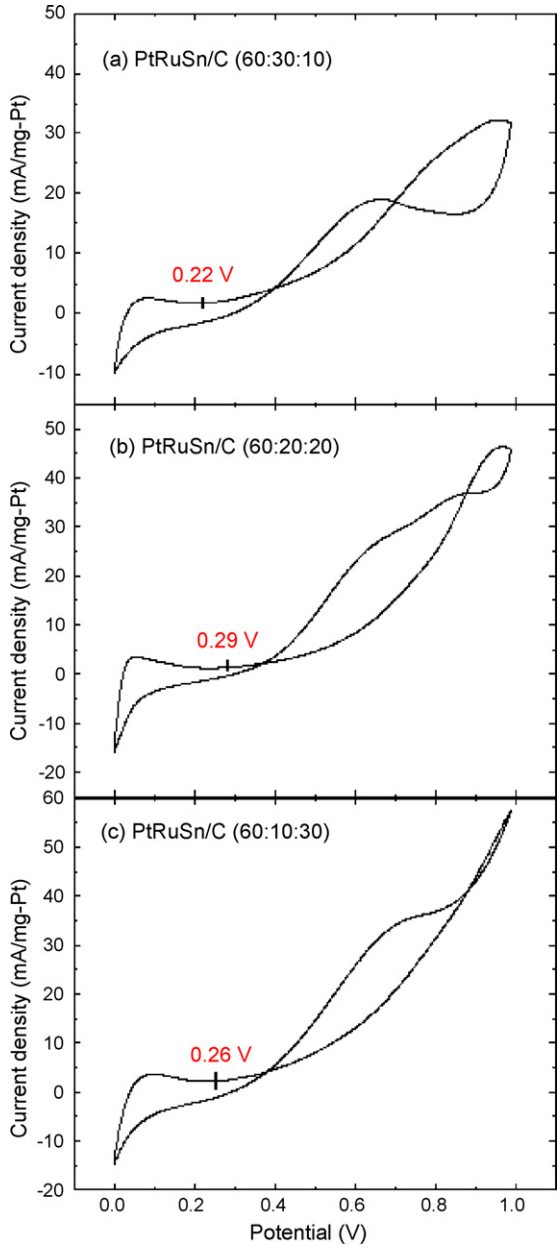

Fig. 4. Cyclic voltammograms for ethanol oxidation on PtRuSn/C catalysts with various atomic ratios: (a) 60:30:10, (b) 60:20:20 and (c) 60:10:30 in 0.5 M CH_3CH_2OH + 0.5 M H_2SO_4 solution, recorded at a sweep rate of 10 mV s^{-1}.

to an insufficient number of Ru sites effectively available as well as to the lack of Pt_3Sn alloy structures to assist the oxidation of adsorbed intermediates. In principle, regarding ethanol adsorption onto and dissociation from Pt sites, the onset potential is related to the breaking of C–H bond and subsequent removal of C_1 or C_2 intermediate by oxidizing with OH_{ad} supplied by adjacent Ru or Sn atoms. At low potential, as compared with Sn, Ru more easily activates H_2O to supply the OH_{ad}, thereby enhancing the tolerant ability for surface poison onto PtRuSn/C catalysts. For the same reason, PtRu is the most suitable catalyst for methanol oxidation. However, in the case of ethanol oxidation, the mechanism and process became more complicated as the activity for ethanol oxidation not only depends on the ability of the respective catalyst for oxidative removal of poisoning adsorbed intermediates such as CO_{ad} or $CH_{x,ad}$ species, but also in particular on its activity for C–C and C–H bond breaking. It can be seen from the CV curves that the highest current density (mass activity, mA mg^{-1} Pt) is not observed over the Ru-rich catalyst (60:30:10), but over the Sn-rich one (60:10:30). This observation that higher Sn content in PtRuSn/C catalyst can generate higher current density during the overall reaction can be explained by two grounds: (i) the ethanol C–C bond scission is effectively activated by forced stretching due to the incorporation of Sn atoms with a higher lattice parameter [25] and (ii) the bonded Pt–C_1 and Pt–C_2 state can be become weak at the boundary between Pt and Sn increasing the turnover frequency of acetaldehyde and/or acetic acid formation, known products of ethanol electrooxidation [33]. The hypothesis that the activation of the ethanol C–C bond depends on Sn addition is quite controversial, despite supporting evidence provided by on-line differential electrochemistry mass spectrometry (DEMS) and IR spectroscopy. Recently, Jusys and coworkers [21] revealed that the addition of Ru or Sn in binary Pt catalysts just can lower the onset potential for ethanol electrooxidation. It does not, however, increase the selectivity for complete oxidation to CO_2 and incomplete ethanol oxidation still prevails on these binary catalysts. In general, the controversies governing the roles of Sn or Ru in C–C bond activation are derived from the differences in experimental conditions regarding ethanol concentrations, temperatures and especially the compositions of the catalysts. Because Pt is now the only metal capable of alcohols adsorption and dehydrogenation at room temperature, energy factors relating to bond cleavage along with geometric factors are sensitive to the composition of the catalyst. If the amount of Ru or Sn added into Pt exceed a limit, it is obvious that the decrease of the Pt content in particles will lower the density of Pt sites available for C–C bond activation and breaking.

In addition, it should be noted that the shapes of the CV curves for ethanol electrooxidation were dependent upon the Ru and Sn ratios in the PtRuSn/C catalysts. In the electrooxidation of ethanol on Pt, there are two peaks during the forward sweep ascribed to the two kinds of oxidation by chemisorbed oxygen species and only one peak in the reversed sweep attributed to renewed oxidation of the ethanol [12]. As for the Ru-rich PtRuSn/C catalyst (60:30:10), the curve shape also seem to contain two peaks in forward scanning at the higher potential region while the Sn-rich PtRuSn/C catalyst (60:10:30) just shows one dominant anodic peaks. The absence of the second oxidation peak in the Sn-rich catalyst can be interpreted as the inability of a Sn-rich surface to transfer oxygen at relatively high potentials as compared with the Ru-rich surface. Moreover, by comparing the current density in forward and reversed scanning, at low potential (0.3–0.6 V), it also was found that the current densities in the reversed scanning for all samples is higher than the counterparts in the forward scanning. At high potentials (0.7–0.9 V), however, the relative contents of Ru and Sn are significant. As for the Ru-rich PtRuSn/C catalyst (60:30:10), the reversed scanning-current density is obviously lower than the forward one. However, with increasing Sn content, the difference in current density between reversed and forward scanning became

more insignificant. Particularly, the reversed current showed the same values as the forward current on Sn-rich PtRuSn/C catalyst (60:10:30). The interesting comparisons reveal that at high potentials, contribution of Sn species in PtRuSn catalyst is helpful in refreshing the active Pt surface and supplying enough Pt sites for ethanol adsorption and dissociation. As for the Ru-rich PtRuSn/C catalyst, passivation of the Pt electrode at higher potential would most likely be observed during the electrooxidation process, probably due to the reversible formation of Ru oxide species which inhibits adsorption of ethanol on Pt sites. A similar passive behavior on PtRu/C catalyst was also reported in the methanol oxidation determined by electrochemical impedance spectroscopy (EIS) [34]. On the other side, at the low potential, Ru species on the surface of the catalysts are more useful than Sn, and can supply oxygen-containing species for the oxidative removal of CO and CH_3CO species adsorbed on adjacent Pt active sites, decreasing the onset potential and enhancing the activity for ethanol electrooxidation.

3.3.2. Electrooxidation of acetaldehyde

It has been generally accepted that the acetaldehyde and acetic acid are two main products in the ethanol electrooxidation. Hence, to further investigate the effect of Ru and Sn content in PtRuSn/C catalyst on the ethanol oxidation process, the electrooxidations of acetaldehyde and acetic acid were studied over these PtRuSn/C catalysts.

The CV curves of acetaldehyde electrooxidation in the 0.25 M CH_3CHO + 0.5 M H_2SO_4 solution recorded on PtRuSn/C catalysts are shown in Fig. 5. According to the CV curves, the hydrogen adsorption/desorption are greatly depressed by acetaldehyde adsorption onto the catalysts, especially in the case of Ru-rich PtRuSn/C catalyst, which is due to an enhanced H_2 evolution based on MS analysis [35,36]. Moreover, the electrooxidation of acetaldehyde can effectively occur on all three PtRuSn/C samples. The highest mass activity (mA mg^{-1} Pt) and the lowest onset potential were observed on the Ru-rich PtRuSn/C catalyst (60:30:10). Similar to the oxidation of ethanol, when the Ru contents further decrease, the onset potential positively shifts from 0.2 V for 60:30:10 to 0.34 V for 60:10:30. However, unlike the oxidation of ethanol, Sn-rich PtRuSn/C catalyst (60:10:30) does not show the highest current density of acetaldehyde electrooxidation at high potentials. Because strong adsorption of acetaldehyde onto the Pt surface almost completely inhibits the hydrogen adsorption, the adsorbed coverage onto the catalyst can reach the limited value which it is sufficient to hinder further C–C bond breaking and CO_{ad} formation but without influence on the partial oxidation of acetaldehyde to acetic acid. It has also been reported [35–37] that in the acetaldehyde electrooxidation over Pt alloy catalysts, acetic acid is the dominant product determined by in situ infrared reflectance spectroscopy, which CO_2 can be almost negligible. The enhancements toward acetaldehyde oxidation by addition of Ru or Sn into Pt are mainly attributed to the effective removal of C_2 species and inhibition of poison formation. They do not involve the C–C breaking. Therefore, by supplying oxygen-containing species that oxidize the acetaldehyde adsorbate (C_2), Ru is obviously superior to Sn.

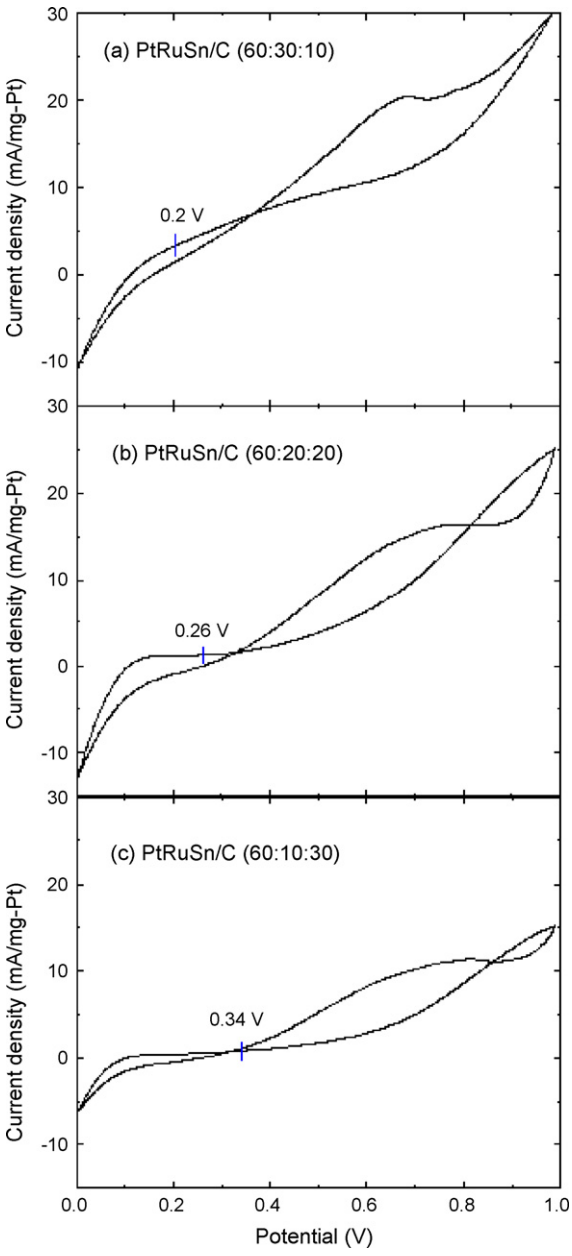

Fig. 5. Cyclic voltammograms for acetaldehyde oxidation on PtRuSn/C catalysts with various atomic ratios: (a) 60:30:10, (b) 60:20:20 and (c) 60:10:30 in 0.25 M CH_3CHO + 0.5 M H_2SO_4 solution, recorded at a sweep rate of 10 mV s^{-1}.

3.3.3. Electrooxidation of acetic acid

Acetic acid is another major product of the electrooxidation of ethanol and further oxidation of acetic acid involving C–C breaking is the critical factor to promote the complete oxidation of ethanol to CO_2. Hence, to further understand the roles of Ru and Sn played in the C–C bond cleaving, electrooxidations of acetic acid were compared over the three PtRuSn/C catalysts.

In order to determine the onset potential and oxidation current during the acetic acid oxidation, the CV curves in the 0.25 M CH_3COOH + 0.5 M H_2SO_4 and 0.5 M blank H_2SO_4 solutions on each PtRuSn/C catalyst were recorded at a sweep rate of 10 mV s^{-1} and room temperature and were compared in Fig. 6. The measured currents are normalized in terms of mass activity

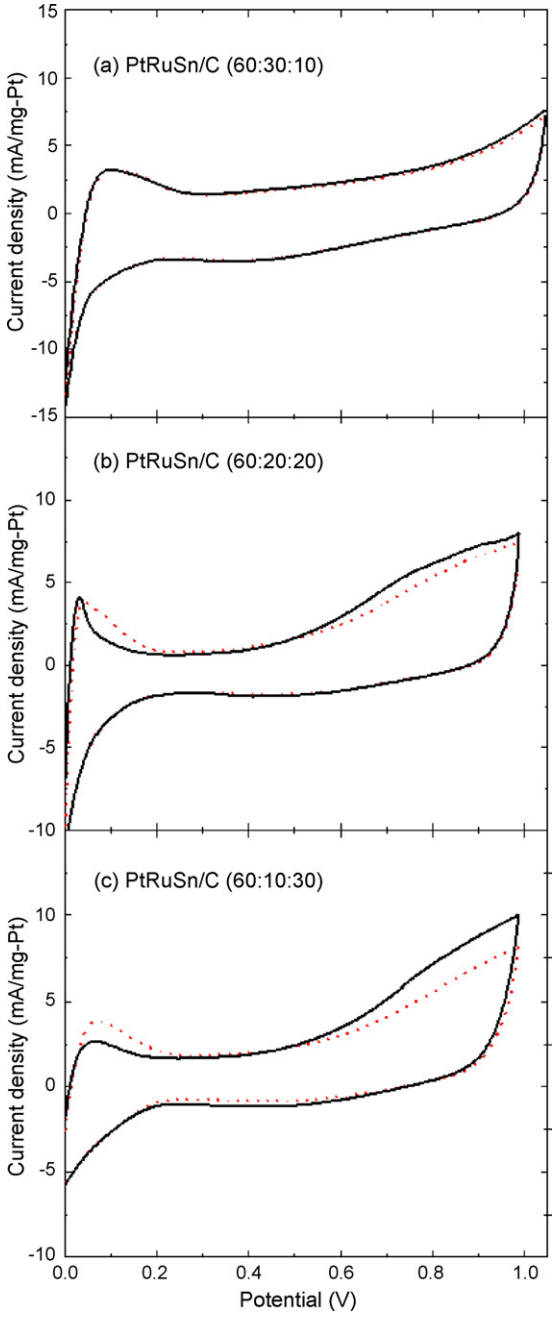

Fig. 6. Cyclic voltammograms for ethanol oxidation on PtRuSn/C catalysts with various atomic ratios: (a) 60:30:10, (b) 60:20:20 and (c) 60:10:30 in 0.25 M $CH_3COOH + 0.5$ M H_2SO_4 solution, recorded at a sweep rate of 10 mV s^{-1}. The dashed lines refer to the curves in 0.5 M H_2SO_4 solution.

(mA mg^{-1} Pt). It can be shown from the results that the Ru-rich PtRuSn/C catalyst (60:30:10) exhibits little current related to the acetic acid oxidation, which is in agreement with recent results reported by Comninellis and coworkers [38]. They synthesized the boron-doped diamond supported $Pt_{80}Ru_{10}Sn_{10}$ catalyst via the microemulsion route and indicated the ternary Pt/Ru/Sn nanoparticles do not show any oxidation for acetic acid. They therefore exhibited no activation in C–C bond scission. However, in our case, when we further increased the Sn contents in the catalyst, the PtRuSn/C catalyst (60:20:20) starts to oxidize acetic acid at 0.55 V and continues with a slightly increasing oxidation current. As for the Sn-rich PtRuSn/C catalyst (60:10:30), it exhibited an onset potential of 0.50 V with a gradually increasing current until the upper-limit potential. These results reveal that in comparison with Ru, Sn plays a very important role in the activation of C–C bonds and hence oxidation of the acetic acid to C_1 species. The ternary PtRuSn catalysts with optimized composition can effectively improve the oxidation of ethanol by enhancing the activity in breaking C–C bonds.

4. Conclusion

Well-dispersed PtRuSn nano-particles with varying atomic ratios (60:30:10, 60:20:20 and 60:10:30) were synthesized and then deposited onto the carbon supports using the alcohol reduction and subsequent heat treatment under Ar–H_2(5%) atmosphere. It was found that the Pt_3Sn phase has a dominant presence in the Ru-rich PtRuSn/C catalyst (60:30:10), while the PtSn phase and SnO_2 were mainly detected in the Sn-rich PtRuSn/C catalyst (60:10:30) showing the larger particle size. The difference in structure and particle morphology among various PtRuSn/C catalysts leads to different electrocatalytic activity for CO stripping as well as the electrooxidations of ethanol, acetaldehyde and acetic acid. Regarding the oxidations of adsorbed CO and ethanol, the Ru-rich PtRuSn/C catalyst (60:30:10) exhibited the lowest onset potential, revealing that the contribution of oxidative removal of the intermediate C_1 and C_2 species from the Pt sites is mainly due to the Ru and the Pt_3Sn alloy structures. However, for the overall oxidation of ethanol, the Sn-rich PtRuSn/C catalyst (60:10:30) containing PtSn and SnO_2 structure are favorable for the activation of the C–C bond, thereby generating higher current density (mass activity) at higher potential. Because of the strong adsorption of acetaldehyde onto Pt sites, as witnessed by depression of the H_2 adsorption/desorption peaks, the oxidation of acetaldehyde is depended on the removal of C_2 intermediates and primarily forms acetic acid. Therefore, as expected, the Ru-rich PtRuSn/C catalyst (60:30:10) significantly enhances the catalytic activity compared with the other PtRuSn/C catalysts. On the other hand, regarding the electrooxidation of acetic acid, remarkable improvement in the oxidation of acetic acid to C_1 species was observed in the Sn-rich PtRuSn/C catalyst (60:10:30), while the Ru-rich PtRuSn/C catalyst (60:30:10) was almost incapable of breaking C–C bonds to oxidize acetic acid. The ternary PtRuSn/C catalyst, benefited from the Ru and Sn simultaneously, shows better performance in the oxidative removal of C_1 and C_2 species at relatively low potentials as well as in the activation of the C–C bonds at high potentials, thereby enhancing the complete oxidation of ethanol. Further optimization of the ternary PtRuSn/C in structure and morphology can be expected to generate highly efficient electrocatalysts for ethanol oxidation in advanced DEFC.

Acknowledgements

The authors acknowledge the financial support of this work from Postdoctoral Science Foundation (2004035300) of China.

We appreciate Prof. Boqing Xu in Tsinghua University for his advice and discussions. We also thank Ms. Tricia H. Kilgore, Ms. Julia G. Colson in South Carolina and Mr. Andy Cavanaugh in Maryland for their kind helps to edit the text.

References

[1] C. Lamy, A. Lima, V. LeRhun, F. Delime, C. Coutanceau, J.M. Leger, J. Power Sources 105 (2002) 283.
[2] S. Rousseau, C. Coutanceau, C. Lamy, J.M. Leger, J. Power Sources 158 (2006) 18.
[3] F. Vigier, S. Rousseau, C. Coutanceau, J.M. Leger, C. Lamy C, Top. Catal. 40 (2006) 111.
[4] A. Demirbas, Prog. Energy Combust. Sci. 33 (2007) 1.
[5] T. Lopes, E. Antolini, F. Colmati, E.R. Gonzalez, J. Power Sources 164 (2007) 111.
[6] S.Q. Song, P. Tsiakaras, Appl. Catal. B: Environ. 63 (2006) 187.
[7] J.W. Long, R.M. Stroud, K.E. Swider-Lyons, D.R. Rolison, J. Phys. Chem. B 104 (2000) 9772.
[8] J.M. Leger, S. Rousseau, C. Coutanceau, F. Hahn, C. Lamy, Electrochim. Acta 50 (2005) 5118.
[9] H. Wang, Z. Jusys, R.J. Behm, J. Phys. Chem. B 108 (2004) 19413.
[10] N. Fujiwara, K.A. Friedrich, U. Stimming, J. Electroanal. Chem. 472 (1999) 120.
[11] G.A. Camara, R.B. de Lima, T. Iwasita, J. Electroanal. Chem. 585 (2005) 128.
[12] M.Y. Wang, J.H. Chen, Z. Fan, H. Tang, G.H. Deng, D.L. He, Y.F. Kuang, Carbon 42 (2004) 3257.
[13] E.V. Spinace, A.O. Neto, M. Linardi, J. Power Sources 124 (2003) 426.
[14] A.O. Neto, M.J. Giz, J. Perez, E.A. Ticianelli, E.R. Gonzalez, J. Electrochem. Soc. 149 (2002) A272.
[15] F. Colmati, E. Antolini, E.R. Gonalez, J. Electrochem. Soc. 154 (2007) B39.
[16] G. Sine, G. Foti, Ch. Comninellis, J. Electroanal. Chem. 595 (2006) 115.
[17] L. Jiang, G. Sun, S. Sun, J. Liu, S. Tang, H. Li, B. Zhou, Q. Xin, Electrochim. Acta 50 (2005) 5384.
[18] E.V. Spinace, M. Linardi, A.O. Neto, Electrochem. Commun. 7 (2005) 365.
[19] F. Vigier, C. Coutanceau, F. Hahn, E.M. Belgsir, C. Lamy, J. Electroananl. Chem. 563 (2004) 81.
[20] F. Colmati, E. Antolini, E.R. Gonzalez, J. Power Sources 157 (2006) 98.
[21] H. Wang, Z. Jusys, R.J. Behm, J. Power Sources 154 (2006) 351.
[22] J.P.I. de Souza, S.L. Queiroz, K. Bergamaski, E.R. Gonzalez, F.C. Nart, J. Phys. Chem. B 106 (2002) 9825.
[23] D.M. Anjos, K.B. Kokoh, J.M. Leger, A.R. De Andrade, P. Olivi, G. Tremiliosi, J. Appl. Electrochem. 36 (2006) 1391.
[24] G.A. Rimbu, C.L. Jackson, K.J. Scott, Optoelectron. Adv. Mater. 8 (2006) 611.
[25] W. Zhou, Z. Zhou, S. Song, W. Li, G. Sun, P. Tsiakaras, Q. Xin, Appl. Catal. B: Environ. 46 (2003) 273.
[26] L. Colmenares, H. Wang, Z. Jusys, L. Jiang, S. Yan, G.Q. Sun, R.J. Behm, Electrochim. Acta 52 (2006) 221.
[27] A.O. Neto, T.R.R. Vasconcelos, R.W.R.V. Da Silva, M. Linardi, E.V. Spinace, J. Appl. Electrochem. 35 (2005) 193.
[28] M. Arenz, V. Stamenkovic, B.B. Blizanac, K.J. Mayrhofer, N.M. Markovic, P.N. Ross, J. Catal. 232 (2005) 402.
[29] V. Radmilovic, T.J. Richardson, S.J. Chen, P.N. Ross Jr., J. Catal. 232 (2005) 199.
[30] A. Kabbabi, R. Faure, R. Durand, B. Beden, F. Hahn, J.M. Leger, J. Electroanal. Chem. 444 (1998) 41.
[31] J.W. Long, K.E. Swider, C.I. Merzbacher, D.R. Rolison, Langmuir 15 (1999) 780.
[32] W.J. Zhou, B. Zhou, W.Z. Li, Z.H. Zhou, S.Q. Song, G.Q. Sun, Q. Xin, S. Douvartzides, M. Goula, P. Tsiakaras, J. Power Sources 126 (2004) 16.
[33] T.E. Shubina, M.T.M. Koper, Electrochim. Acta 47 (2002) 3621.
[34] G. Wu, L. Li, B.Q. Xu, Electrochim. Acta 50 (2004) 1.
[35] K.B. Kokoh, F. Hahna, E.M. Belgsir, C. Lamya, A.R. de Andrade, P. Olivi, A.J. Motheoc, G. Tremiliosi-Filho, Electrochim. Acta 49 (2004) 2077.
[36] H. Wang, Z. Jusys, R.J. Behm, J. Appl. Electrochem. 36 (2006) 1187.
[37] J.L. Rodriguez, E. Pastor, X.H. Xia, T. Iwasita, Langmuir 16 (2000) 5479.
[38] D. Siné, M. Smida, G. Limat, Ch. Comninellis, J. Electrochem. Soc. 154 (2007) B170.